

Preliminary Conceptual Analysis for a Multiplexed Reflectometry Beamline at SNS

Frank Klose and John Ankner
Oak Ridge National Laboratory
June 21, 1999

Prepared for the SNS Instrument Oversight Committee
SNS document ES-1.1.8.4-6015-RE-A-00

Content:

- I. Overview
- II. Figure of the reflectometry beam line
- III. General design choices
 - a) Liquids reflectometer features
 - b) Magnetism reflectometer features
 - c) Common features
- IV. Table of parameter values
- V. Instrument performance
 - a) Resolution and Q-range
 - b) Simulation of the instruments
 - c) Data rates
- VI. Summary

Appendixes:

- A. Technical drawings
- B. A neutron channel guide bender as wavelength and background filter
- C. Redesign of the shutter area and layout of the beam tubes
- D. Simulation of the optical components by acceptance diagrams
- E. Data rate estimates
- F. Research and development projects related to the instruments

I. Overview

The proposed reflectometry beamline consists of two separate instruments sharing the same beamport, one specialized in soft matter/liquids experiments and the other in magnetism.

The first instrument is designed to study the reflectivity of horizontal surfaces. Due to its vertical scattering plane it can accommodate liquid surfaces (Figure 1 provides a schematic representation, and chapter IV gives the parameters for this instrument). The instrument will be useful for a wide range of science, including interfacial studies in polymers and surface chemistry involving thin layers of surfactants or other materials on the surfaces of liquids. Data rates and Q-range covered at a single scattering angle setting will be sufficiently high to permit "real time" kinetic studies on many systems. Time resolved experiments include investigations of chemical kinetics, solid state reactions, phase transitions, and chemical reactions in general.

The magnetism reflectometer is designed to examine (solid) thin films and superlattices, especially in regard to their magnetic properties. The scattering plane has been chosen horizontal to allow more convenient operation of the instrument and auxiliary equipment. As can be seen in Fig. 1, (and in detailed drawings in the appendix) the polarized reflectometer sample position is significantly farther away from the moderator than that of the liquid instrument, allowing diffraction experiments complementary to reflectometry. Besides the conventional capability of a neutron reflectometer to analyze the structural and magnetic depth profiles of thin film structures, complementary kinetic studies, for example in order to examine the dynamic behavior of magnetic domains, are feasible. The capability of "time-tagging" pulses over a broad Q-range to study processes with longer time constants (msec to hours) is unique to the TOF method and should be explored. Furthermore, studies of phonons and magnons at interfaces might become reality with this instrument (see chapter IV for detailed instrument parameters).

Both instruments will have independent views of the moderator and neutron guide systems. The instruments are physically separated by 4° horizontally and 2° vertically and further by means of two channel-guide benders installed inside the main shutter. These allow in addition a 2.5° vertical deflection in the beam direction of the liquids instrument and a 2° horizontal deflection for the case of the magnetism reflectometer, resulting in a vertical and horizontal separation of > 1 m at a distance of 11 m from the moderator. This design offers the advantage that the neutron wavelength spectrum used in the experiment ($\lambda > 2.5 \text{ \AA}$) can be separated from the fast neutron and γ radiation of the prompt pulse far upstream.

The performance of the instruments has been calculated in comparison with the IPNS reflectometers. It is estimated that data collection time can be reduced from 24 h periods down to the magnitude of minutes (see appendix E for details).

II. Figures of the reflectometry beam line

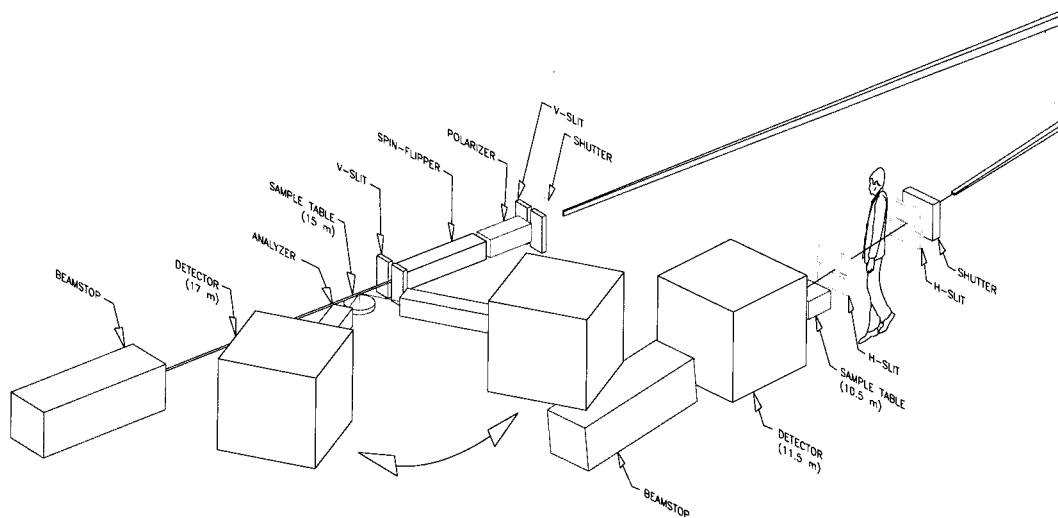
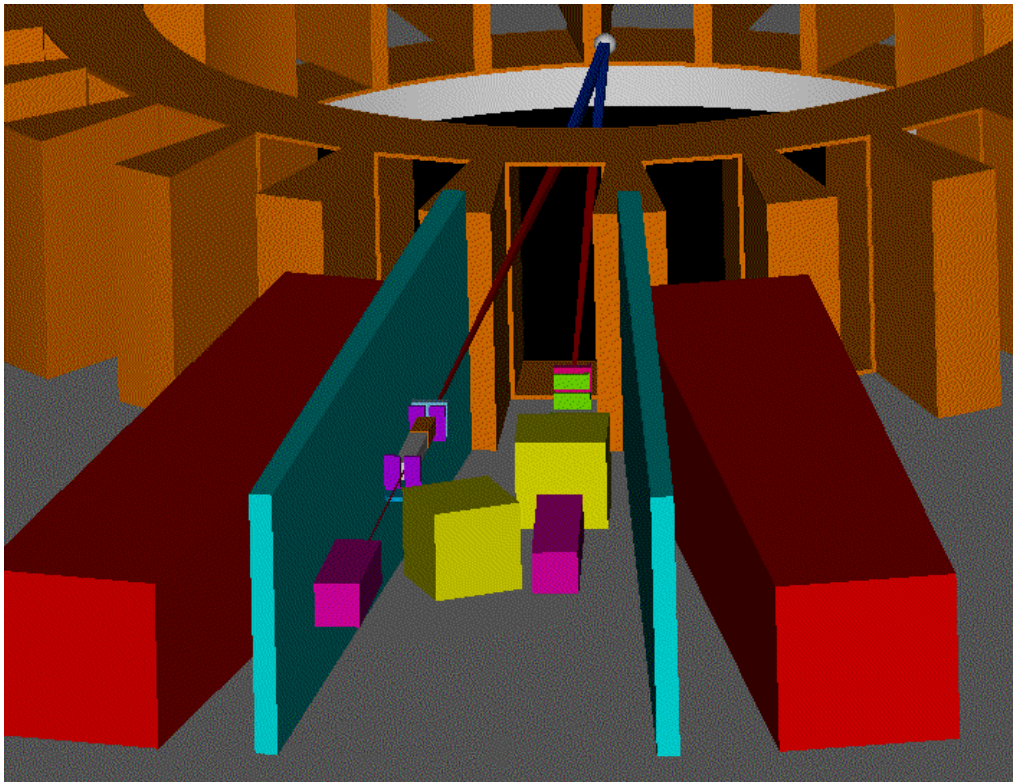


Figure 1

- a) 3dim. representation of the reflectometry beamline
 (the upper instrument is the magnetism reflectometer, the lower one the liquids reflectometer)
 Note that the detector of the magnetism instrument can easily swing over the liquids instrument's beam stop



- b) 3dim. representation of the reflectometry beam line, view from the detectors towards direction of the moderator
 (left: magnetism instrument with horizontal scattering plane, right: liquids instrument with vertical scattering plane, the red blocks represent shielding requirements around the neighboring beam lines)

III. General design choices

a) Liquids reflectometer features

A reflectometer designed to measure liquids must operate without inclination of the sample surface, yet span a sufficient Q range to resolve thin adsorbed layers. Traditional instruments employ one of two approaches to satisfy these constraints. Fixed-wavelength instruments tip the monochromator slightly out of its scattering plane to alter the angle of incidence onto the sample, which is raised and lowered to intercept the deviated beam. Broadband instruments, such as those at spallation sources, utilize a very broad wavelength band at a single fixed angle of incidence onto the surface. We propose a hybrid instrument that makes use of the moderate wavelength band available at the 60 Hz SNS and a widely divergent beam emerging from a tapered supermirror guide. This instrument couples the flexibility of incident-angle variation with the efficiency of broadband data collection.

The centroid of the beam emerging from the tapered guide will be inclined at an angle of 4.5° to the sample surface. This deflection is comprised of an initial 2° downward inclination from the moderator and an additional 2.5° deflection by a microguide bender located in the beamline shutter ($2.5 \text{ m} < l < 4.5 \text{ m}$). The microguide bender eliminates direct line-of-sight of the moderator and allows us to dispense with a t_0 chopper, resulting in lower background. In addition, without having to absorb the high-energy neutrons in the direct line-of-sight, we can use separate beam shutters external to the target monolith for independent operation of the two instruments.

The most important aspect of this instrument is the production of a broad angular range of neutrons by the tapered guide (see Appendix D for details of the neutron optics). Fig. 2 shows this distribution for 14-Å neutrons. At this wavelength, by aligning slits at the appropriate angle, we can observe beams over a ± 100 mradian ($\pm 5.7^\circ$) range. The angular range depends on λ and the taper angle of the guide,

$$\Delta\gamma = \pm(c\lambda + \chi^{\text{taper}}).$$

Using $4\theta_c^{\text{Ni}}$ guide coatings ($c = 6.92 \text{ mradian}/\text{Å}$), the angular range varies from ± 29 mradian (3 Å) to ± 105 mradian (14 Å). The quality of the guide coatings critically affects performance, as shown by the color-coded plots ranging from an average reflectivity of 1 (red) to 0.85 (green). By placing the center of this angular distribution at 4.5° , we can cover a range of incident angles $0 < \gamma_1 < 9^\circ$. In a typical measurement of a liquid sample, one begins at the left of the distribution with tight collimation, accumulates data in the available wavelength band, resets slits and sample height, and collects data at a deeper angle with more relaxed collimation, etc. It will be possible to cover a range of Q out to 0.5 Å^{-1} in 5-10 settings. Wavelength bandwidth-shifting choppers provide added flexibility. Note that the widths of individual peaks in the angle distribution average about 10 mradian (0.6°) and are piled together in places to a total width of 30 mradian. We can use a significant fraction of this divergence at high Q values, where $\delta\theta/\theta$ as large as 10-15% might be acceptable. Measurements on solid samples will generally be made at the centroid position, utilizing maximum wavelength bandwidth and variation of the sample tilt angle.

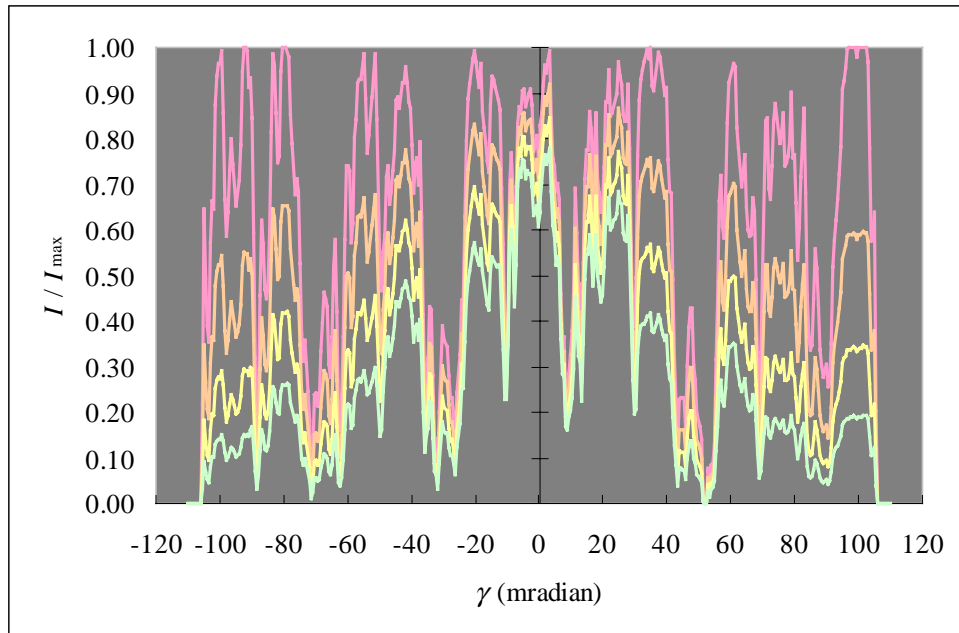


Figure 2: Intensity fraction of full illumination for 14-Å neutrons plotted as a function of exit angle relative to $4\theta_c^{\text{Ni}}$ tapered guide center line. Since different angular divergences correspond to different numbers of reflections in the guide system, the average reflectivity of the guides critically affects the performance of the instrument. The red curve assumes reflectivity of 1, orange 0.95, yellow 0.90, and green 0.85.

b) Magnetism reflectometer features

The magnetism reflectometer detector will be placed at a distance of 17 m. The instrument will have the unique capability to perform (under the same experimental conditions) high-angle diffraction in addition to the conventional reflectometry experiments. Combining these two techniques in one instrument will allow one to link structural and magnetic properties existing on the dimension of film thickness with properties on atomic length scales. Naturally, this instrument will be equipped with spin polarizing/analyzing supermirror or ^3He devices. The polarized neutrons will eventually allow incorporating a Drabkin-type neutron energy filter for high wavelength resolution capabilities.

Polarizers/analyzers

Currently we are favoring stacked supermirror systems as polarizing and analyzing elements. Preferably supermirrors of the FeCo/Si design (HMI Berlin) shall be used since they allow working in transmission geometry. This mode of operation is much more convenient, since after insertion/demounting of the mirrors, the beamline does not need to be realigned. Using transmission supermirrors will allow a very rapid change between a polarized (or polarization analysis) mode and an unpolarized mode. Due to the rather high divergence of the incoming beam, it will be necessary to stack at least two cassettes of mirrors at a different angle relative to the nominal beam direction in an accordion-like arrangement behind each other. We have recently initiated a research program together with Thomas Krist, HMI Berlin to develop a new concept for unlimited neutron bandwidth supermirror polarizers (see Ref.1).

It is most likely that the ^3He polarizer technique will make major improvements over the next years. This technique will particularly enhance the capability to analyze the spin of neutrons which are scattered in a rather broad angular range (for example when diffuse scattering takes place). We are involved in a research project of Mike Snow, Indiana University. Test experiments of polarized ^3He used for spin analyzing purposes will take place at the POSY1 reflectometer in fall of 1999.

Neutron spin flipper

As neutron spin flipper it is planned to use a so-called "Drabkin-monochromator" [2]. Besides the capability to reverse the spin-state of the neutrons, this device may allow the reshaping of the wavelength distribution of the neutron pulse at a given time. The analogue to this device for a reactor-based instrument would be a monochromator with electronically tunable wavelength resolution. The Drabkin-flipper will finally allow tuning the time-resolution in the experiments without changing the length of the instrument (the device is described in the appendix/R&D projects).

c) Common features

Source

A partially coupled supercritical hydrogen moderator at $\sim 22\text{K}$ on beamline 15TD provides a polychromatic beam of cold neutrons to the instruments. The design documented here assumes a fwhm pulse width of $\delta t \approx 210 \mu\text{s}$ at 10 \AA , $\delta t \approx 90 \mu\text{s}$ at 5 \AA , $\delta t \approx 50 \mu\text{s}$ at 3 \AA , and $\delta t \approx 15 \mu\text{s}$ at 1 \AA [3]. The instrument is located on beamline 15TD which is specialized to accommodate the separate neutron guide tubes for the two instruments. The partially coupled cold moderator was selected for the reflectometry beamlines because of the high intensities at long wavelengths. Pulse widths are only moderately important for these instruments.

Choppers

T_0 choppers for cutting out the background from the prompt pulse are not used in the current concept since we eliminate direct line-of-sight to the moderator by deflecting the beam. A series of bandwidth-limiting choppers is required to limit the incident bandwidth to prevent frame overlap. To provide maximum flexibility, this series of choppers must be able to select different bandwidths as well as to vary the wavelength at which the incident bandwidth is centered. The requirement to vary the selected bandwidth can be satisfied by using two choppers. This bandwidth can be centered at any wavelength simply by adjusting the phase of the bandwidth choppers. The second chopper, when properly positioned, can also help to cut out additional neutrons that could contaminate the data.

It should be noted that there might be a possible contamination of certain wavelengths ($\lambda = (h \cdot n \cdot f) / (m \cdot L)$, where h : Planck's constant, n : frame number, f : source frequency, m : neutron mass, L : instrument length) due to the background created by the prompt pulse. For the liquids reflectometer located 11.5 m from the moderator, the prompt pulse affects adversely $\lambda = 5.99 \text{ \AA}$, 11.98 \AA , 17.96 \AA etc. For the magnetism reflectometer at 17 m, $\lambda = 3.87 \text{ \AA}$, 7.75 \AA , 11.62 \AA , 15.50 \AA etc. is affected. If the prompt pulse background turns out to be a significant problem, these wavelength numbers should be chosen as nominal borders for the frames.

Optimization of the chopper locations and speeds will be described in a forthcoming technical document (a spreadsheet tool has already been developed by J.K. Zhao).

Neutron guide system

The two reflectometers will have independent but fairly similar guide systems (schematic as well as scaled drawings can be found in the appendix). Both guides use the full moderator face of 12 cm height and 10 cm width (and not a small stripe only) because a large divergent beam must be transported to the instruments to keep a constant relative resolution function feasible at high scattering angles. The most important task of the guide system is to eliminate the direct line-of-sight to the moderator as far upstream as possible. This will be achieved by redirecting the beam from its original direction (a 2.5° downwards deflection for the case of the liquids reflectometer and a 2.0° horizontal deflection away from the liquids beamline for the case of the magnetism reflectometer). The approach we have examined in detail uses a channel bender device. After the beam exits the bender, the neutrons are vertically and horizontally focused onto the sample by means of a $4\theta_C$ Ni tapered neutron guide. The exit dimensions of the tapered guides are matched to typical sample sizes (≈ 5 cm in the uncollimated direction, ≈ 2 cm in the collimated direction).

The channel beam benders

Two channel beam benders will be used for achieving enough separation between the two instruments. However, just as important is that the device filters the incoming neutron spectrum. It will bend only neutrons of a certain minimum wavelength. By bending the polarized beamline away from the direct beam emerging from the moderator by about 2° , we lose direct line-of-sight already after 8.5 m. Thus, a "clean" neutron beam, essentially free of fast neutron and γ radiation contributions will be delivered to the sample.

Inspecting possible locations for a bending device, the most attractive one is inside the main shutter of the beamline, which begins 2.5 m from the moderator. The shutter offers 2 m space along the neutron flight path and is relatively easily accessible in case the bender needs to be replaced after years of operation. The bender itself consists of double-side supermirror coated glass (or Si plates) stacked onto each other with separating vacuum gaps of some millimeters. They are arranged in a segment of a circle (or in several straight parts with different angles as an approximation) and guide the neutron beam through the vacuum channels. For achieving mechanical stability, the substrates need to be about 1 mm thick. Typical channel width will be about 10 mm (a schematic drawing of the bender device can be found in the appendix). Neutron channel beam benders of similar design have already been built (e.g. at NIST) and they function properly.

In view of the high radiation levels present at SNS, the long-term stability of the supermirror coatings is certainly a technical risk, which needs to be examined in the near future (see R&D projects).

Main beam shutter redesign

We have proposed to the target systems group a design for implementing the multiplexed beam line approach. The main difference compared to the old design is that the shutter needs to be much wider in order to accommodate two neutron guides. Due to its general relevance for the whole SNS instrumentation, these results have been presented at the Target/Instrument group meeting (Oak Ridge, April 16, 1999). The concept has been positively evaluated and will be presented as a major redesign proposal to the SNS management.

Drawings of the modified neutron beam shutter area can be found in the appendix.

Collimation

A sequence of two computer-controlled slits (located after the exit of the converging guide) will be used at each instrument to define the final angular resolution used in the experiments. For a typical sample geometry, the beam will be a few mm high and several cm wide. For the case of the liquids instrument it is planned that the nominal downwards inclination of 4.5° (relative to the horizontal) can be changed $\pm 4^\circ$ by using the divergence in the beam. This permits scattering angle changes during reflectivity experiments from horizontal surfaces (e.g., free liquid surfaces).

Sample

The sample stages are provided with automated rotational and translational motions. For the case of the liquids reflectometer, the entire assembly sits atop a vibration isolation mount. The shielded room that contains the final collimation slit, the sample, and the detector is environmentally controlled. Due to spatial constraints caused by the close proximity of the two beamlines, it may be necessary to operate the instruments from a platform above them.

Detectors

The detectors are placed on automated mounts to allow adjustment of height, distance from sample, and tilt of the detector. A 2dim. PSD is used to provide the necessary angular resolution and a convenient operation of the instrument. Today's choice would possibly be a ^3He wire detector. However, technology is improving in this field and the final decision for the detector should be delayed as long as possible.

It should be mentioned here, that the expected instantaneous count rate in worst cases (direct beam measurements or measurements of a sample in the region of total reflection) can be as high as 300000 counts/sec over the whole detector or 100000 counts/sec/cm² in the spot of the reflected beam. This is beyond the capabilities of today's detectors and is a focal point of our R&D program.

IV. Table of parameter values

Table 1: Reflectometry beam line instrument parameters.

Similar/common instrument components (for each instrument)	Parameter	Value	Cost (\$1000)
Beam line	Beamport	15TD	
Source	Nominal instrument frequency	60 Hz	
Moderator	Location	Upper/downstream	
	Type	Liquid H ₂ (partially coupled)	
t_0 chopper	(will be replaced by a	channel bender device)	
Bandwidth chopper		TBD	
Collimation	Before sample	Variable apertures	
Sample	Surface area	50 - 2500 mm ²	
Position-sensitive detector (eac	Type	TBD	
	Area	40 cm x 40 cm	
	Distance from sample	0.5 - 3 m	
	Position resolution	≈ 1 mm	
	Quantity	2	
Scattering chamber	Geometry	TBD	
Sample alignment	Goniometer (external to chamber)	2 circle	
	Translations	X, Y, Z movements	
Beam-line shielding	Steel radial thickness around beam	0.7 m	
	Paraffin radial thickness around steel	0.2 m	
	Length	up to ≈ 9 m from moderator	
Beam stop	Steel	0.5 m x 0.5 m x 1.5 m	
	Paraffin radial thickness around steel	0.2 m	
Data acquisition		Standard system	

Components for liquids reflectometer	Parameter	Value	Cost (\$1000)
Geometry	Source-sample	10.5 m	
	Sample-detector	1 - 3 m	
	Scattering plane	vertical	
Channel beam bender	Aperture (height/width)	120 mm / 100 mm	
	Distance from moderator (begin, end)	2.5 m < l < 4.5 m	
	Bending angle	2.5° (downwards)	
	Coating	3 - 4 θ_C Ni coating	
	Cut-off wavelength	3 Å	
Neutron guide	Tapered guide	(horizontal and vertical)	
	Coating	4 θ_C Ni	
	Distance from moderator	4.5 m < l < 8.5 m	
	Initial aperture (height/width)	120 mm / 100 mm	
	Final aperture	17.5 mm / 50 mm	
Sample angles (on liquids)	$\theta_{\min} - \theta_{\max}$	1° - 8°	
Wavelength-range (typical)	$\lambda_{\min} - \lambda_{\max}$	4.0 Å - 9.8 Å (at 60 Hz)	
Q-range	$Q_{\min} - Q_{\max}$	$\approx 0 - 0.5 \text{ \AA}^{-1}$	
Resolution	$\Delta Q / Q$	1% - 10%	

Components for magnetism reflectometer	Parameter	Value	Cost (\$1000)
Geometry	Source-sample	15.0 m	
	Sample-detector	1 - 3 m	
	Scattering plane	horizontal	
Channel beam bender	Aperture (height/width)	120 mm / 100 mm	
	Distance from moderator (begin, end)	2.5 m < l < 4.5 m	
	Bending angle	2.0° (horizontal)	
	Coating	3 - 4 θ_C Ni coating	
	Cut-off wavelength	2.5 Å	
Neutron guide	Tapered guide	horizontal and vertical	
	Coating	4 θ_C Ni	
	Distance from moderator	4.5 m < l < 12.5 m	
	Initial aperture (height/width)	120 mm / 100 mm	
	Final aperture	20 mm / 50 mm	
Polarizer	Supermirror	FeCo/Si	
Analyzer	Mode	Transmission	
	Supermirror	FeCo/Si	
	Mode	Transmission	
	(optional: Drabkin type)	^3He	
Spin flipper	Drabkin type	2	
Wavelength-range (typical)	$\lambda_{\min} - \lambda_{\max}$	4.0 Å - 8.0 Å (at 60 Hz)	
Q-range	$Q_{\min} - Q_{\max}$	$\approx 0 - 5 \text{ \AA}^{-1}$	
Resolution	$\Delta Q / Q$	1 % - 10 %	

V. Instrument performance

a) Resolution and Q-range

The parameter of interest for reflectometry is the normal wave-vector transfer Q_z given by

$$Q_z (\text{\AA}^{-1}) = \frac{4\pi \sin \theta}{\lambda (\text{\AA})} = \frac{4\pi L(m) \sin \theta}{3955.4(m \cdot \text{\AA} / s)t(s)}$$

The resolution in this variable is given approximately by

$$\frac{\delta Q_z}{Q_z} = \left\{ \left(\frac{\delta t}{t} \right)^2 + \left(\frac{\delta L}{L} \right)^2 + (\cot \theta \delta \theta)^2 \right\}^{1/2}$$

i.e. for large angles of incidence the beam should be quite divergent in order to illuminate the sample with maximum intensity (and also to be able to control the resolution over a wide range). Due to this reason, highly reflecting guide coatings should be used. The goal should be to transport a beam divergence of 1 - 2° through the guide.

Also of interest are the minimum and maximum values of Q_z that can be reached. These are given by

$$Q_{z-\min/\max} = \frac{4\pi \sin \theta_{\min/\max}}{\lambda_{\max/\min}}$$

It can be seen that there is no significant problem in reaching a sufficient large Q-range for the case of the magnetism reflectometer, since the scattering angle and the wavelength band used in the experiment can be shifted relatively easy. The $Q_{z-\max}$ is limited by the highest scattering angle 2θ ($\approx 160^\circ$) and the minimum neutron wavelength which is transported through the neutron guides ($\lambda_{\min} \approx 2.5 \text{\AA}$). These values result in $Q_{z-\max} = 4.95 \text{\AA}^{-1}$. The value for $Q_{z-\min}$ is not severely limited for this instrument.

For the case of the liquids reflectometer the angle of incidence can be varied from 0° to 9° by sampling the intensity distribution emerging from the tapered guide, allowing us 0\AA^{-1} to 0.5\AA^{-1} in Q. For solid samples, one can tilt the sample surface and access whatever Q-range is needed. We are currently investigating the impact of the various angular and wavelength distributions in the tapered guide beam on data collection.

b) Simulation of the instruments

We have implemented an acceptance diagram formalism on Excel spreadsheets for instrument simulation (see appendix D for an example of the liquids instrument).

c) Data rates

Data rate calculations for the instruments have been carried out in comparison with the POSY1 reflectometer from IPNS. Gains/losses from the different neutron sources, the moderators, the neutron guides and from geometrical factors have been considered. We estimate that the SNS reflectometers will accumulate data 400 -500 times faster than the IPNS reflectometer, compressing 24 h runs into several minutes of data collection. However, reflectometry at SNS

will not only be faster, but the quality and the Q-range of the data will be orders of magnitude better compared to IPNS.

The details of the calculations are given in the appendix.

VI. Summary

In summary, both instruments are rather complementary, since they emphasize different aspects of the neutron reflectivity technique. The liquids reflectometer will feature high-intensity, broad band, high speed data collection, medium Q-resolution and horizontal sample surface capabilities. In contrast, the magnetism beamline will accentuate polarized neutron, reflectivity/diffraction, high wavelength/Q-resolution and low background capabilities.

The neutron guide design approach presented in this proposal could have a major impact on the design of the remaining SNS instrumentation since it points out potentialities to multiplex beamlines in order to enhance the number of instruments in the limited space available. Furthermore, we present a channel beam bender device as an alternative to the use of T_0 choppers for the purpose of wavelength filtering and background radiation reduction.

We want to point out that for the reflectometry beam line no severe compromises in design choices have been made due to the fact that two instruments occupy the same beam port. The instruments would be designed very similarly if one would have two separate beam ports available. Thus, multiplexing instruments is a very promising approach for SNS instrumentation design.

However, the changes in beamline geometry required to implement two independent views of the moderator have not yet been incorporated in the project baseline. We plan to seek such approval this summer.

Appendixes:

A. Technical drawings

Additional technical drawings are attached. These include the following plans:

- side view of the reflectometry beam lines
- top view of the reflectometry beam lines
- side view of the shutter area (including built in channel beam deflector)
- outline of the guide system for the liquids reflectometer neutron guide system (side view)
- outline of the guide system for the magnetism reflectometer neutron guide system (top view)

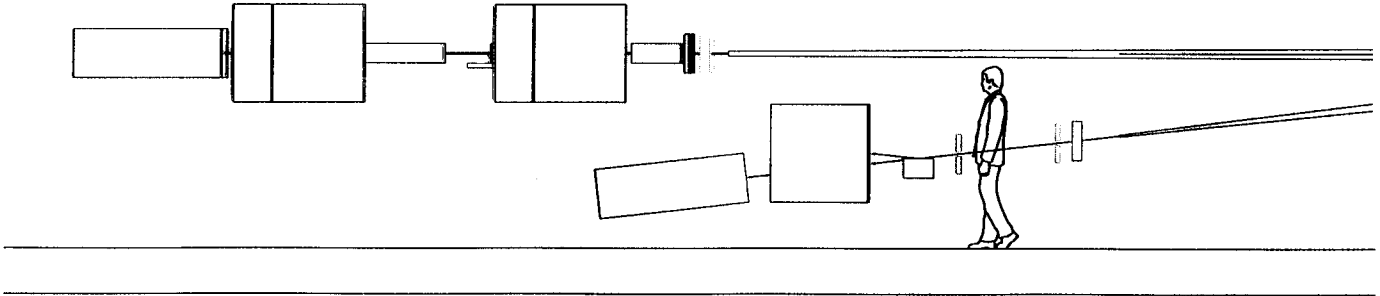


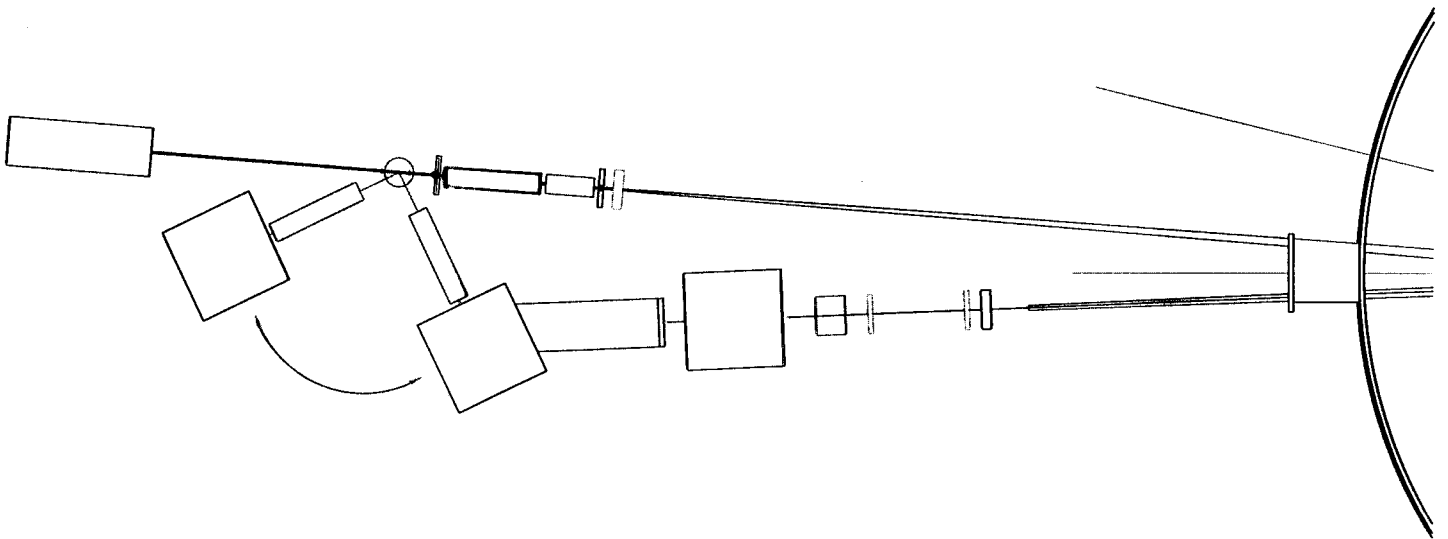
Figure A1

a) Side view of the beam lines

The upper beam line is the magnetism reflectometer with the detector shown in two different situations, one typical for reflectometry experiments, the other typical for diffraction.

The lower inclined beam line is the liquids reflectometer.

(Note that due to the inclination of the liquids reflectometer's guide there is sufficient space between the magnetism reflectometer's detector and the beamstop of the other instrument.)



b) Top view of the reflectometry beam lines

Also for this case, the magnetism reflectometer's detector is shown in two different positions.

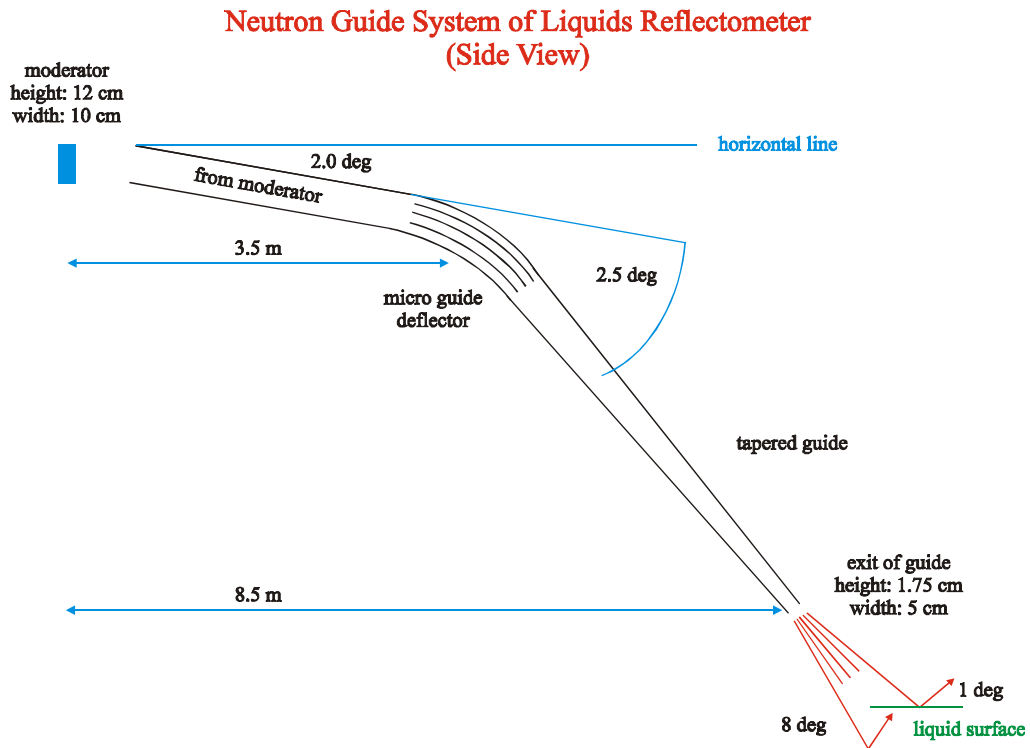
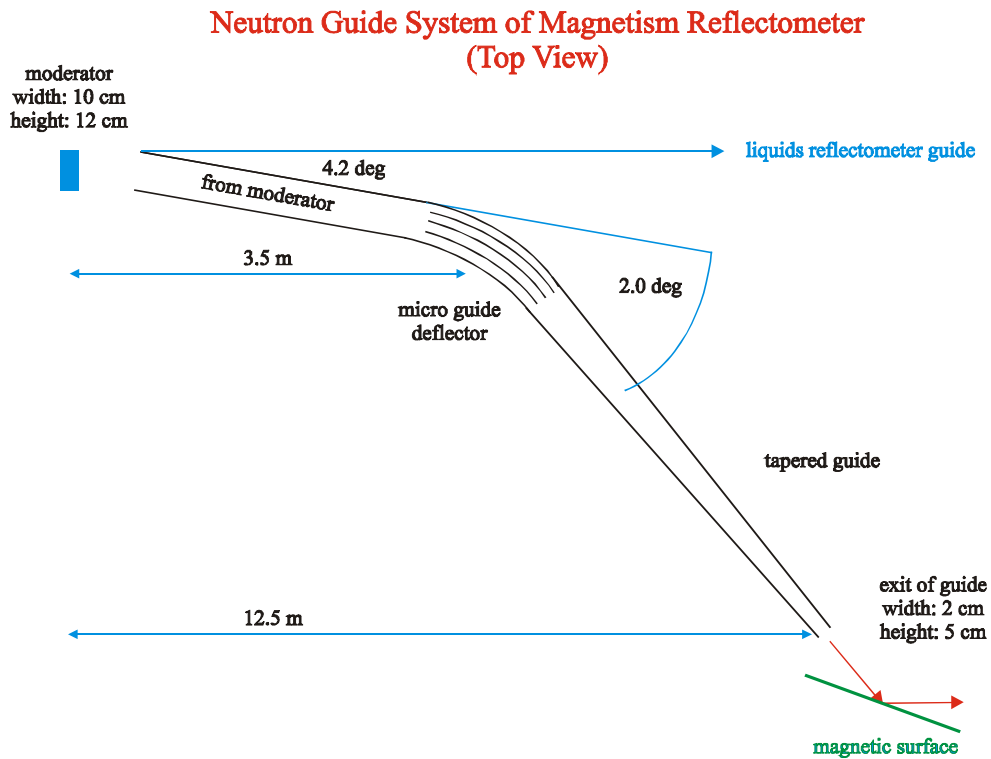


Figure A2

a) outline of the guide system for the liquids reflectometer neutron guide system (side view)



b) outline of the guide system for the magnetism reflectometer neutron guide system (top view)

B. A neutron channel guide bender as wavelength and background filter

In a first approximation, we assume an ideal device, which is homogeneously illuminated by a source located immediately in front of the entrance of the bender. For such a device the wavelength dependence of the transmission through the device is characterized by the cut-off wavelength λ_C , the characteristic deflection angle β and the critical angle of the guide coating per unit wavelength γ_C [4]. The geometrical design, i.e. the channel width s and the radius R enters into β . The relations are: $\lambda_C = \beta \cdot \gamma_C^{-1} = \gamma_C^{-1} \cdot (2s/R)^{1/2}$. For the liquids reflectometer the channel width will be 6.2 mm, λ_C will be 3.2 Å for a 3m supermirror coating (3 times the critical angle of natural Ni) and $\lambda_C = 2.4$ Å if a 4m coating is used. For the magnetism reflectometer the channels will be 4.9 mm wide, $\lambda_C = 3.8$ Å for 2m coating and $\lambda_C = 2.5$ Å for 3m coating. From the relation between the substrate thickness and the channel width, it can be seen that 80% (or more) of the neutron flux is accepted by the devices. Besides the theoretical transmission function of the device, one also needs to consider transmission losses due to imperfect reflectivity of the guide coatings. It can be shown that reflectivity losses are at a minimum in the region of the characteristic wavelength. Thus, the wavelength band between λ_C and $2 \cdot \lambda_C$ offers optimal neutron transmission and should be chosen for the majority of the experiments.

The illumination geometry for the bender will be different for our experimental setup. The main difference is that the bender is located 2.5 m away from the moderator. Thus, the device needs to be reevaluated by means of the acceptance diagram technique. Since the blades of the device cannot be expected to stop 1 GeV neutrons, our final configuration will likely differ somewhat from the treatment above.

This approach will significantly lower the background and is more promising than using a T_0 chopper since the available volume for blocking the direct high-energy beam is an order of magnitude higher. Since direct line-of-sight to the moderator is completely lost already after ≈ 8.5 m, the two instruments can be operated independently by means of two separate thermal neutron beam shutters.

C. Redesign of the shutter area and layout of the beam tubes

Upon being asked to investigate the possibility of implementing two reflectometers on one beam line, we concluded that if both instruments were to receive the full useful angular divergence, each must have an independent view of the entire moderator face. This need in turn prompted a re-examination of the configuration of the beam tubes inside the target monolith. We proposed to the Oak Ridge Target Group, during a workshop this past April, a number of modifications to enhance the flexibility of the beamlines.

To achieve 1-m separation of the liquid and polarized beam lines at a distance of 10 m from the moderator, the two lines must diverge by an average of about 5° over their entire length. We propose to implement this separation via an initial 4.2° divergence centered on the moderator face and an additional 2.0° deflection by a microguide bender in the polarized beam line. Installation of two independent beam lines on a single port requires a redesign of the penetrations through the outer reflector, beam line shutter, and external wall of the target monolith in both horizontal (see Fig. C1) and vertical directions (see Fig. C2).

Modification of the shutter is the most technically challenging and potentially expensive requirement of the beamline redesign. Figure C3 shows a possible design. Installation of these wide shutters is physically possible on 8 of the 18 SNS beamlines. The presence of such shutters,

even if not initially required, is an investment in future flexibility. We plan to submit project change requests after the July baseline review to request funds and authorization to proceed with a redesign of some fraction of the beamlines. Our work on installing two reflectometers has catalyzed this effort.

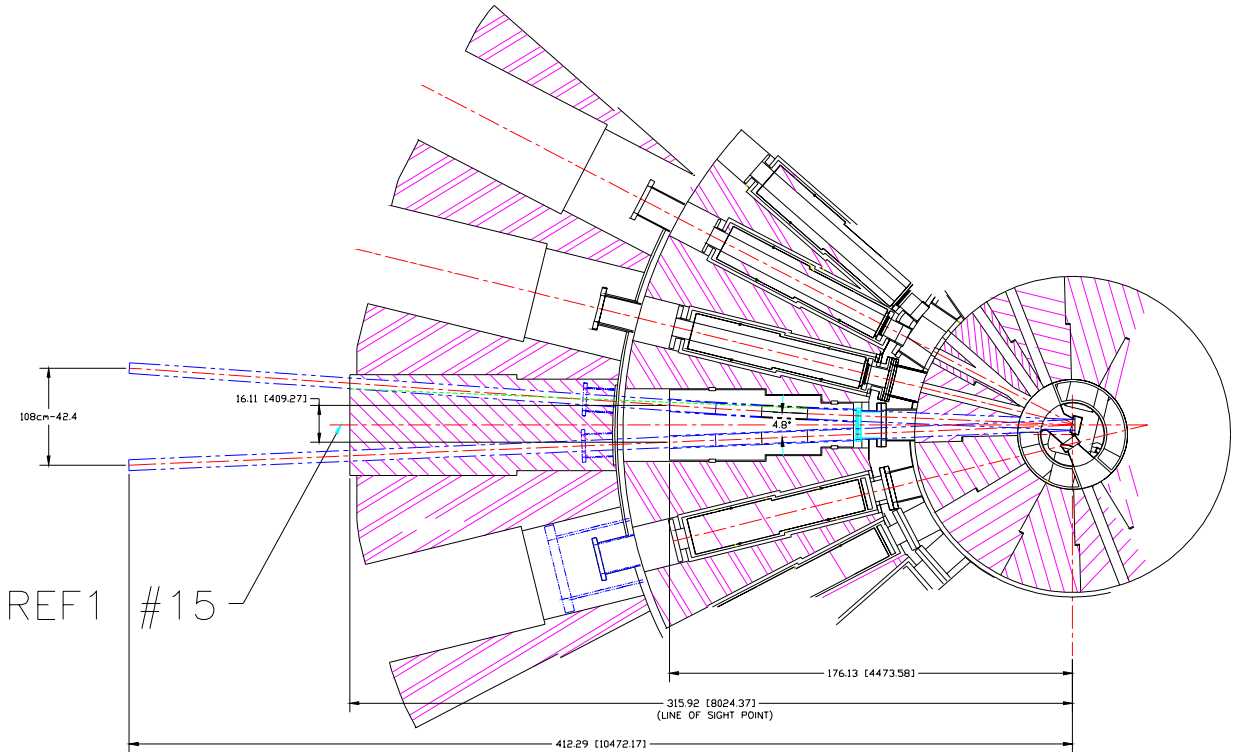


Figure C1: Plan view of proposed beamline modifications needed for installation of two reflectometers.

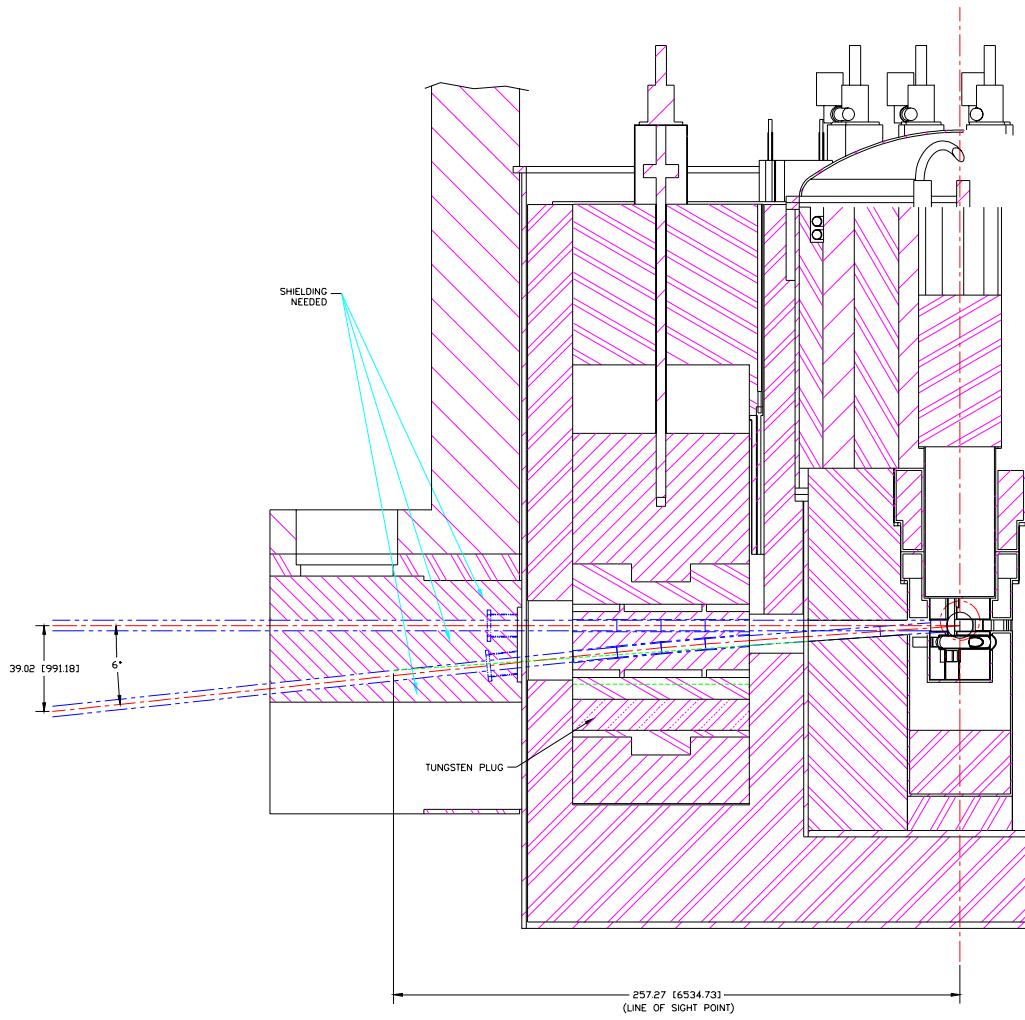


Figure C2: Elevation view of beamline modifications

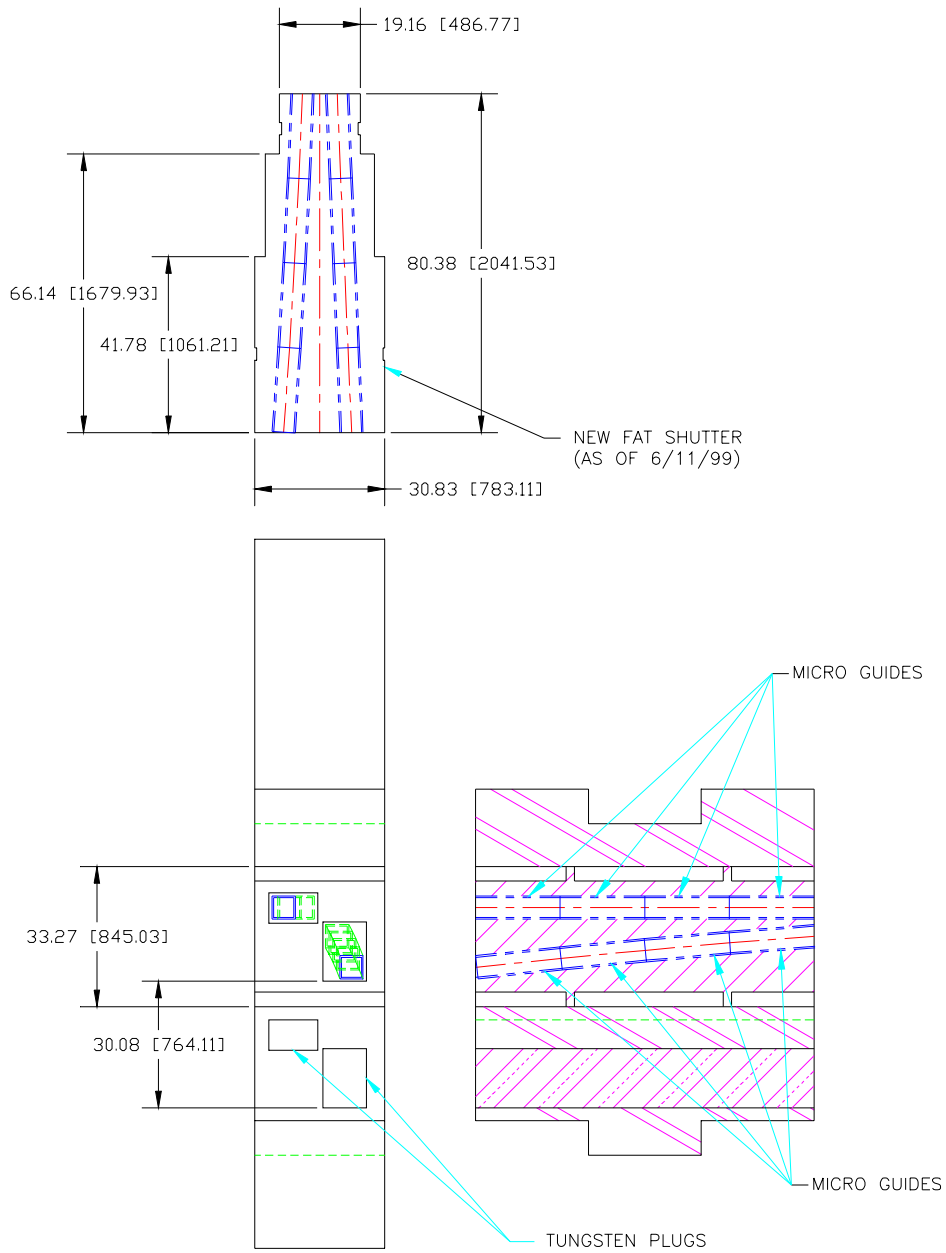


Figure C3: Detail view of proposed thick shutter. These could be installed on as many as 8 of the 18 SNS beamlines.

D. Simulation of the optical components

We have used acceptance diagrams [5,6] implemented in Excel spreadsheets to model the optical performance of the reflectometers and other instruments. The acceptance diagram is a phase-space representation that plots a neutron's spatial coordinate on exit from a guide or other optical component vs. its angular divergence from the centerline. This intensity distribution is passed to the next component in the instrument.

One-dimensional representations are easiest to comprehend and as long as the two spatial components perpendicular to the beam direction are not coupled, one can simply multiply the results. Consider the flux passed by the 2.5-m-long beam tube that views the moderator of the liquids reflectometer. At the exit of this 12-cm-wide tube, one observes the acceptance diagram shown in Fig. D1. The ± 6 cm tube aperture accepts ± 48 mradian angular divergence. Integration of the x coordinate yields the familiar triangular slit angular intensity distribution. The area enclosed by the polygon is proportional to the flux.

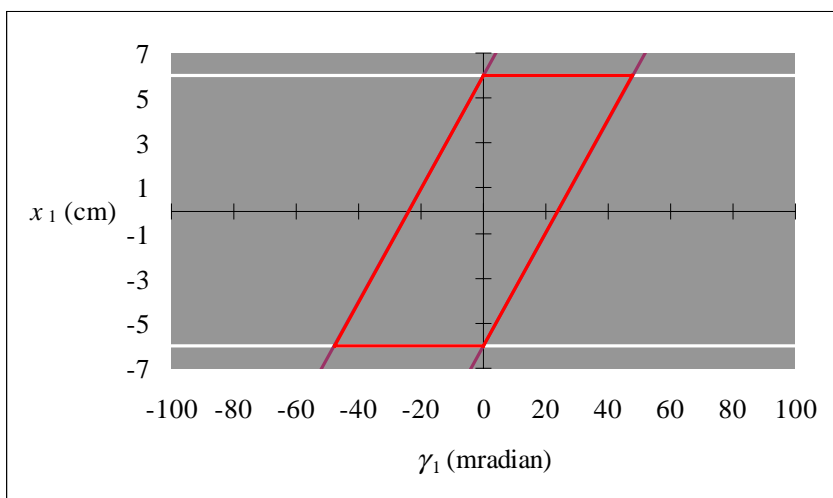


Figure D1: Exit acceptance of 2.5-m-long, 12-cm-wide liquids reflectometer beam tube viewing the moderator. Neutrons of ± 48 mradian can pass through.

The beam next passes into a four-segment circular microguide bender device [7] that both eliminates line-of-sight (in conjunction with the tapered guide) and deflects the beam downward by 2.5° . The 50-cm-long segments consist of 6 2-cm-wide channels separated by Si wafers coated on both sides with $4\theta_c^{\text{Ni}}$ supermirror. Each segment is offset 11 mradian with respect to the preceding optical element.

In order to eliminate line of sight of the moderator, one must treat the Si channel separators as transparent to highly energetic neutrons (energies up to 1 GeV). To such neutrons the microguide looks just like a 12-cm beam tube. The acceptance diagram at the exit of the fourth segment is shown in Fig. D2. As in Fig. D1, the area within the red polygon contains the phase-space coordinates of the neutrons emerging from the bender. Clearly, we have not eliminated the line-of-sight neutrons. However, if we now pass these neutrons into a tapered guide (12 cm to 1.75 cm over 6 m length) offset by 11 mradian, we can send all of these neutrons into the wall of the guide (see Fig. D3). The x coordinate of the tip of the polygon corresponds to interception of this least-favorable beam by the wall of the tapered guide 1.4 m from its exit, thus eliminating

line-of-sight and providing some distance to absorb the neutrons (much greater than the 30 cm allotted to a t_0 chopper).

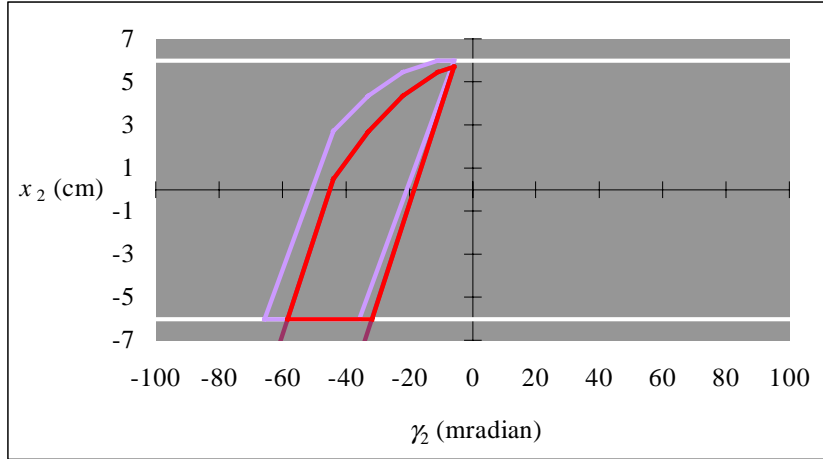


Figure D2: Acceptance diagram of high-energy neutrons at exit of four-element bender. Note that all of the neutrons have negative angular divergences.

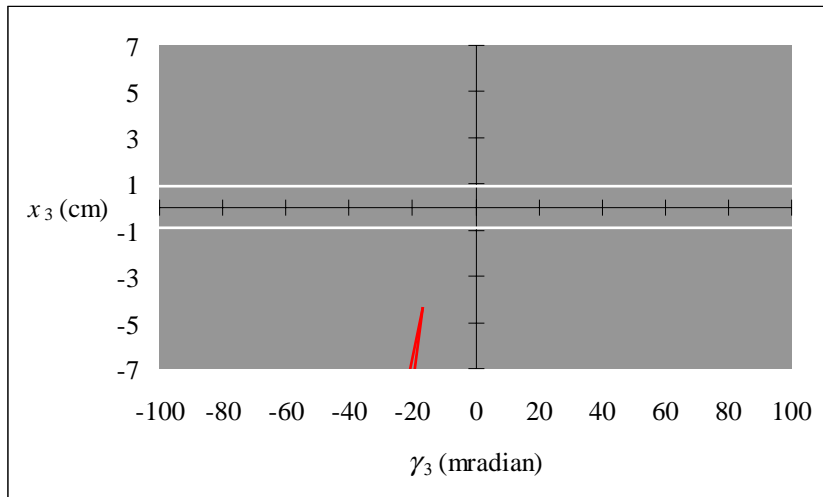


Figure D3: Acceptance diagram at exit of tapered guide, demonstrating interception of direct beam by walls of guide 1.4 m from exit.

The passage of thermal and cold neutrons through the bender is considerably more interesting. Depending on wavelength and divergence, neutrons may be reflected one or more times (see Fig. D4). The white lines show the channel walls, containing distinct populations of neutrons. The blue vertical lines show the critical angles. Red polygons enclose coordinates of 7.5-Å neutrons that don't strike a guide surface, while progressively bluer polygons represent populations of neutrons reflected one or more times. Figure D5 shows the intensity distribution of different reflection indices of neutrons integrated over the 12-cm spatial coordinate in 0.5 mradian bins.

This beam then passes into a tapered guide 6 m long, narrowing from its initial 12 cm width to 1.75 cm at exit. The taper angle of this guide is 8.54 mradian ($\sim 0.5^\circ$). Each successful reflection from the walls adds twice the taper angle to the angular divergence. This effect creates a broad divergent beam, the components of which are shown in Fig. D6 below, along with the in-

tensity sum corrected for guide average reflectance (Fig. D7). Since the neutrons may reflect many times in transit through the guide system, high reflectance coatings are a necessity.

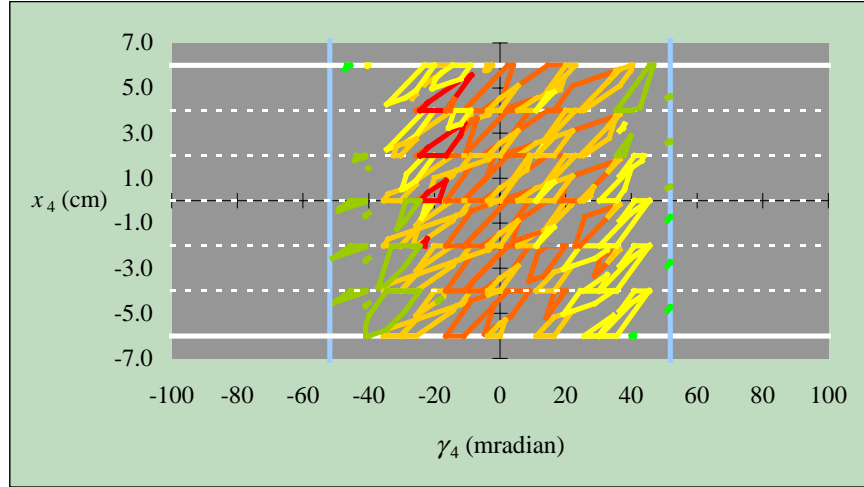


Figure D4: Neutrons (7.5 \AA) exiting the bender reflected 0 (red), 1 (orange), 2 (gold), 3 (yellow), 4 (lime), and 5 (green) times. The pale blue vertical lines show the critical reflection angles and the white lines outline the 6 bender channels.

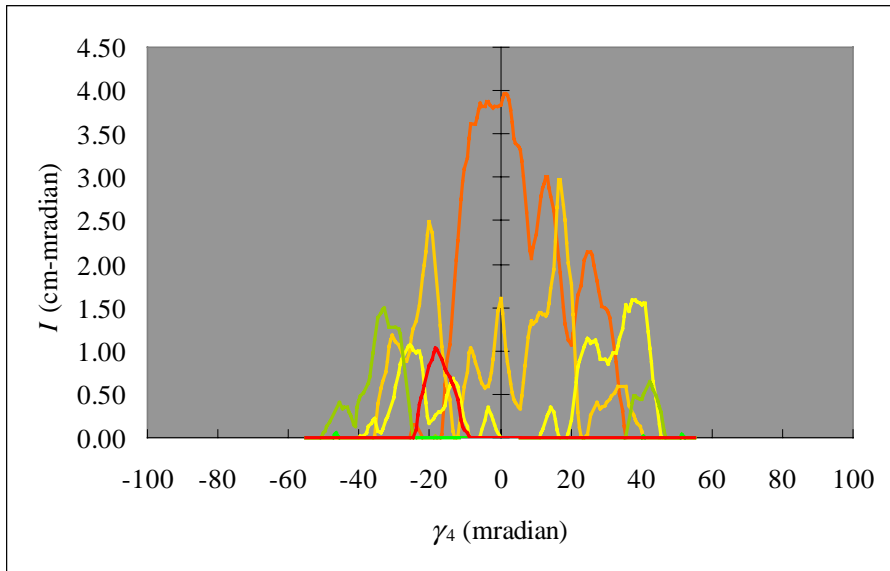


Figure D5: Intensity integrated over the spatial coordinate in 0.5 mradian bins. Full illumination corresponds to $12 \text{ cm} \times 0.5 \text{ mradian} = 6 \text{ cm} \cdot \text{mradian}$.

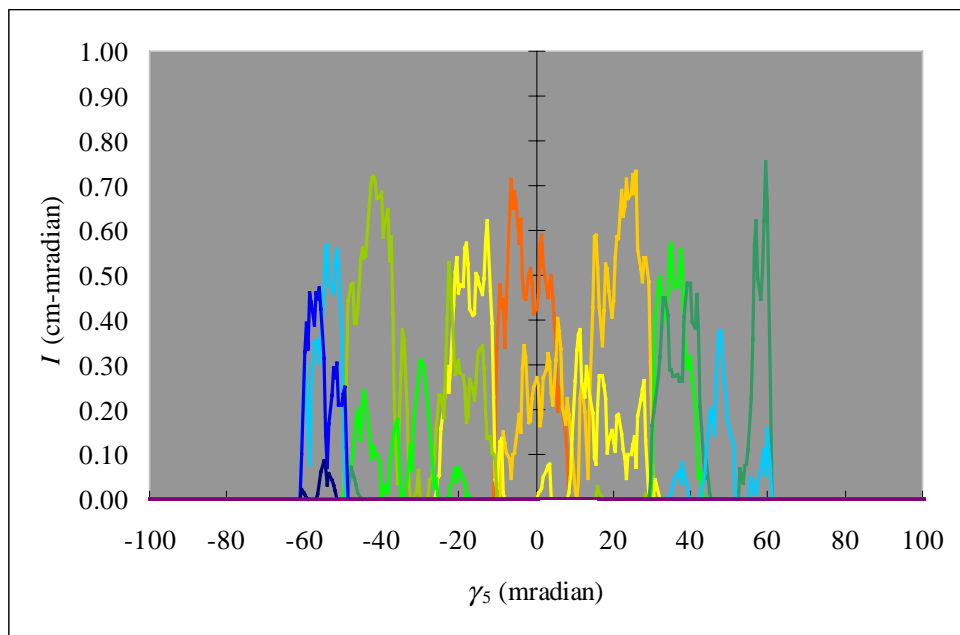


Figure D6: Intensity distribution of 7.5-Å neutrons exiting from the tapered guide, again integrated over spatial coordinate (1.75 cm) in 0.5 mradian bins (maximum intensity 0.875 cm-mradian).

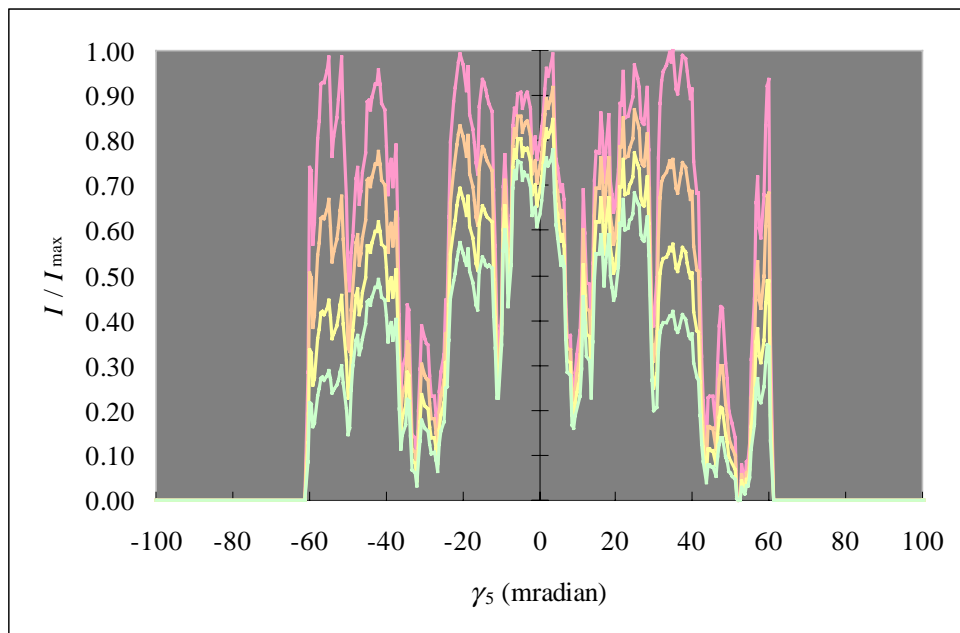


Figure D7: Reflectance-weighted integrated intensity as a fraction of full illumination for guide average reflectances 1.00 (red), 0.95 (orange), 0.90 (yellow), and 0.85 (green).

By scanning a two-slit collimator across this intensity distribution, one can access a range of different angles of incidence onto the sample, while utilizing all of the wavelength components present in the beam. We are currently engaged in simulating reflectivity from a realistic sample to determine the optimum angle for the beam centroid.

E. Data rate estimates

Ratio of Target yields (SNS to IPNS)

(taken from Ken Herwigs report)

Estimate of target yields is taken from Eqn. 2.1, pg. 105 of *Methods of Experimental Physics, Neutron Scattering*, Vol. 23, part A.

$$\begin{aligned}\text{Yield} &= 0.1(E_{\text{GeV}} - 0.120)(A + 20) \text{ for all non-fissile materials} \\ &= 50.0(E_{\text{GeV}} - 0.120) \text{ for } ^{238}\text{U}\end{aligned}$$

The expected ratio in neutron yields may then be taken as

$$\text{SNS: } 0.1(1.0 - 0.120)(200 + 20) = 19.4 \text{ neutrons/proton (SNS is a 1 GeV source)}$$

$$\text{IPNS: } 50.0(0.45 - 0.120) = 16.5 \text{ neutrons/proton (IPNS is a 450 MeV source)}$$

The next step is to put in the number of protons/pulse.

IPNS uses a 0.015 mA source with a repetition rate of 30 Hz or has

$$(0.015 \times 10^{-3} \text{ A}) \left(1 \text{ proton} / 1.6 \times 10^{-19} \text{ C} \right) (1 / 30 \text{ s}) = 3.125 \times 10^{12} \text{ protons/pulse}$$

or

$$(16.5 \text{ neutrons/proton}) \left(3.125 \times 10^{12} \text{ protons/pulse} \right) = 5.16 \times 10^{13} \text{ neutrons/pulse}$$

$$\begin{aligned}\text{equivalent proton power on target} &= (450 \times 10^6 \text{ eV}) \left(1.6 \times 10^{-19} \text{ J/eV} \right) \left(0.015 \times 10^{-3} \text{ A} \right) \left(1 \text{ proton} / 1.6 \times 10^{-19} \text{ C} \right) \\ &= 6.75 \text{ kW}\end{aligned}$$

SNS will use a 1 mA source with a repetition rate of 60 Hz or has

$$(10^{-3} \text{ A}) \left(1 \text{ proton} / 1.6 \times 10^{-19} \text{ C} \right) (1 / 60 \text{ s}) = 1.042 \times 10^{14} \text{ protons/pulse}$$

or

$$(19.4 \text{ neutrons/proton}) \left(1.042 \times 10^{14} \text{ protons/pulse} \right) = 2.02 \times 10^{15} \text{ neutrons/pulse}$$

$$\begin{aligned}\text{equivalent proton power on target} &= (1.0 \times 10^9 \text{ eV}) \left(1.6 \times 10^{-19} \text{ J/eV} \right) \left(1.0 \times 10^{-3} \text{ A} \right) \left(1 \text{ proton} / 1.6 \times 10^{-19} \text{ C} \right) \\ &= 1 \text{ MW}\end{aligned}$$

For 2 MW operation the SNS numbers double !

SNS Magnetism Reflectometer

Compare this instrument with POSY1 (located at moderator C2) at IPNS for count rate specs.

Table of Instrument Parameters

	d_{MS} (m)	d_{SD} (m)
POSY1	8.3	0.9
Mag.Ref.	15	2

Expected ratio of neutrons hitting the sample based on the instrument geometry (no guides) is given by:

$$R = \left(\frac{d_{MS}(\text{POSY1})}{d_{MS}(\text{MagRef})} \right)^2$$

where d_{MS} is the moderator-sample distance (Note that the SNS reflectometer has another geometrical advantage at higher scattering angles, because it will view the full moderator surface resulting in higher flux. POSY1 uses only a small stripe of the moderator surface. However, this factor is not included in the calculation).

Using the entries in the table, $R = 0.31$.

In order to estimate count rates, we take a "high" count rate sample (data were taken around the edge of total reflectivity). The sample was a La/Fe multilayer, run Wiebke4041, sample size 4 cm long x 2 cm tall. In the TOF intensity histogram, we see a maximum of 617 counts in a time bin of 158 microseconds accumulated in a total measuring time of 162015 pulses (1.5 h) (at full IPNS power). **Instantaneous count rate** then is given by:

$$I_{\text{POSY1}} = \frac{P}{t_{\text{total}}} \times \frac{1}{F} \times \frac{1}{B}$$

where P is the maximum number of neutron counts in a single time bin, t_{total} is the total run time, F is the repetition rate of the source, and B is the bin width of a single time channel. For this example, $t_{\text{total}} = 1.5$ hr, $F = 30$ pulse/sec, and $B = 158$ microsec, giving $I_{\text{POSY1}} = \mathbf{24.1}$ cps.

Moderator gains (from Erik Iverson):

The magnetism reflectometer will be on the upper downstream liquid hydrogen moderator (beamport 15TD). One can roughly estimate the moderator gain of SNS (in the range of around 5 Å) by applying the following factors: The IPNS C2 moderator (decoupled) gains a factor of 1.7 by the grooved surface. On the other hand the SNS moderator is a partially coupled moderator with a gain factor of 4 relative to the decoupled IPNS C2 moderator (the gain for a fully coupled moderator would be another factor of 2). The numbers results in a total **gain for the SNS moderator of 2.4**.

Guide gains:

In the wavelength range around 5 Å, the gain of the (converging guide) is theoretically about an order of magnitude. However, there are losses due to misalignment, imperfect coating etc. A conservative estimate for the guide gain would be a gain factor of 7.

On the SNS then one could expect to see an **instantaneous count rate** of

$$I_{MagRef} = I_{POSY1} \times 2.4 \times 7 \times 0.31 \times \frac{4.04 \cdot 10^{15}}{5.16 \cdot 10^{13}} \times \left(\frac{d(POSY1)}{d(MagRef)} \right) = 5318 \text{cps}$$

(or 1970 cps/cm² of detector area since the signal is concentrated in an area of 2.7 cm²). The last term in this equation reflects the change in bin width that should be inversely proportional to the total flight path, d , of the respective instruments.

Note that the instantaneous count rate does not depend on the source repetition rate, only on the total number of neutrons generated per pulse.

If one can use the full 60 Hz repetition rate of SNS, one expects the count rate for an equivalent sample will be f times faster per detector than POSY1 where

$$f = \frac{60 \text{ Hz}}{30 \text{ Hz}} \times \frac{6176 \text{ cps}}{24.1 \text{ cps}} = 441$$

At POSY1 a complete reflectivity run with polarized neutrons (reflectivity range: 1 - 10⁻⁴) takes about 24 hours. At SNS we can expect to collect the same data quality in less than 3 minutes.

Caution:

At the SNS reflectometers, we are measuring always close to the maximum intensity of the moderator.

Due to the larger wavelength band used at POSY1 the peak reflectivity of the sample was not matched to the peak of the wavelength distribution of the incoming beam. Matching this would give an additional factor of 50 in peak count rate:

Worst case for SNS reflectometer:

about 300000 counts/sec or 100000 counts/sec/cm²

F. Research and development projects related to the instruments

Radiation damage induced by fast neutron and γ radiation

In view of the planned installation of supermirrors as close as 2.5 m to the moderator, we have already started a collaboration with potential supermirror suppliers (PSI/Villigen and HMI Berlin) for studying survivability of the coatings in high radiation fields. These studies will be carried out at Argonne's Intense Pulsed Neutron Source. Here, we will have an irradiation hole close to the IPNS source region available by late summer 1999.

For the design of the SNS instruments it is very important to get a realistic estimate of the time period over which certain optical components will survive in high radiation fields. Problems of radiation induced damage can especially be expected for the case of high critical angle supermirrors (3 or $4 \times \Theta_c$ of Ni) because these coatings are already under high mechanical strain due to the fabrication process. In worst cases, the mirrors might not only lose some of their favorable optical properties but also completely peel off the substrates. No extended study has been made so far in this regard. The tests on these supermirrors are especially important since supermirror bender devices have the potential to replace T_0 choppers at some SNS beamlines.

Development of a Drabkin neutron energy/wavelength filter prototype at IPNS

This project concerns the development and implementation of a new prototype for a time-of-flight neutron energy filter, which is based on magnetic spin resonance. The analogue to this device for a reactor-based instrument would be a monochromator with electronically tunable wavelength resolution.

In early 2000 we are planning to investigate a new "moderator pulse reshaper" concept for a time-of-flight instrument. The design is not completely new but dates back to an idea of Drabkin (1962) for a resonance spin filter for slow neutrons. It has been described in detail recently for the case of a fixed wavelength instrument [2], but was never, to our knowledge, successfully applied to TOF.

The development of such a device will overcome the most serious drawback related with the use of a high-intensity coupled liquid hydrogen moderator, i.e. the long tail of delayed neutrons. This tail is unfavorable because it degrades the time-resolution of the instrument. The intensity gain factor in using a coupled instead of a decoupled moderator is about 2 to 4 (depending on wavelength).

The pulse reshaper needs polarized neutrons (which can be provided by the POSY1 instrument at IPNS). The basic functioning of the device is that it flips neutrons only if they have a certain wavelength and if they arrive at a certain time. This can be achieved by applying (in addition to a variable external dc guide field) spatially periodic magnetic fields of certain strength and at a certain time. The "good" neutrons (having correct wavelength and arrival time) can be effectively filtered from "bad" neutrons (having either wrong wavelength or wrong arrival time) by a second supermirror. In this way, we can eliminate the delayed neutron "tail" of the moderator emission and, at the same time, eliminate very slow neutrons from the previous pulses. The energy (or wavelength) resolution can be matched to the angular resolution of the experiment (typically 2%) by choosing a suitable number of magnetic field reversals N inside the device ($\Delta\lambda/\lambda \sim 1/N$).

Gian Felcher (ANL/MSD), who has already done some preliminary design for such a device, will take part in this project as scientific advisor. After successful implementation, the prototype will remain permanently mounted at the POSY1 reflectometer.

References

- [1] Th. Krist, F. Klose and G.P. Felcher, *Physica B* **248** (1998) 372.
- [2] M.M. Agamalyan, G.M. Drabkin and V.I. Sbitnev, *Physics Reports*, **168** (1988) 265.
- [3] Erik Iverson, private communication.
- [4] A.A. van Well, *Nuclear Science and Engineering*, **110** (1992) 10.
- [5] J.M. Carpenter and D.F.R. Mildner, *Nucl. Instr. Meth. A* **196** (1982) 341.
- [6] J.R.D. Copley, *Nucl. Instr. Meth. A* **287** (1990) 363.
- [7] D.F.R. Mildner, H.H. Chen-Mayer, G.P. Lamaze, and V.A. Sharov, *Nucl. Instr. Meth. A* **413** (1998) 341.